Research paper

# Mixed-chalcogenide diplatinum complexes; an investigation of ligand exchange processes using ESI mass spectrometry

Ryland G. Fortney-Zirker [a], William Henderson [a,*], Edward R.T. Tiekink [b]

[a] Chemistry, School of Science, University of Waikato, Private Bag 3105, Hamilton 3240, New Zealand
[b] Research Centre for Crystalline Materials, School of Science and Technology, Sunway University, 47500 Bandar Sunway, Selangor Darul Ehsan, Malaysia

ABSTRACT

Routes to mixed-chalcogen diplatinum complexes have been explored using Electrospray Ionisation Mass Spectrometry (ESI-MS) as a powerful technique to probe reaction solutions on the microscale. Exchange reactions of binuclear platinum(II) complexes $[Pt_2(\mu\text{-}E)_2(PPh_3)_4]$ (E = S, **1**; Se, **2**) with each other, or reactions with the elemental chalcogens [viz. complex **1** with Se, and complex **2** with $S_8$] all had limited success in forming the mixed species $[Pt_2(\mu\text{-}S)(\mu\text{-}Se)(PPh_3)_4]$. Reactions of complex **1** with $Ph_2Se_2$ and **2** with $Ph_2S_2$ resulted in the ESI MS detection of novel arylated mixed-chalcogenide complexes $[Pt_2(\mu\text{-}S)(\mu\text{-}SePh)(PPh_3)_4]^+$ and $[Pt_2(\mu\text{-}Se)(\mu\text{-}SPh)(PPh_3)_4]^+$, respectively. The analogous reactions of **1** and **2** with diaryl ditellurides $R_2Te_2$ (R = Ph, $p\text{-}EtOC_6H_4$) resulted in the ESI MS detection of the trinuclear aggregates $[\{Pt(PPh_3)\}_3(\mu_3\text{-}E)(\mu\text{-}TeR)_3]^+$ and the mixed-chalcogenide complexes $[Pt_2(\mu\text{-}E)(\mu\text{-}TeR)(PPh_3)_4]^+$ (E = S, Se; R = Ph, $p\text{-}EtOC_6H_4$). The compound $[\{Pt(PPh_3)\}_3(\mu_3\text{-}Se)(\mu\text{-}TePh)_3]PF_6$ was synthesised on the macroscopic scale, and characterised by elemental analysis and a single-crystal X-ray diffraction study.

© 2017 Elsevier B.V. All rights reserved.

## 1. Introduction

The binuclear platinum(II) sulfide complex $[Pt_2(\mu\text{-}S)_2(PPh_3)_4]$ **1** has been known for a long time [1], and has a well-established, extensive and diverse chemistry, primarily as a result of the high nucleophilicity of the bridging sulfido ligands. This can be exemplified by the reactivity of complexes containing $\{Pt_2S_2\}$ cores towards even very weak alkylating agents such as dichloromethane [2,3]. Closely-related analogues, with alternative phosphine ligands in place of $PPh_3$, are also well-known [4,5]. The related selenide complex $[Pt_2(\mu\text{-}Se)_2(PPh_3)_4]$ **2** has

been less-intensively studied [6], but has distinctive reactivity differences compared to its sulfide counterpart [7–9]. The chemistry of these complexes, which has been reviewed on a number of occasions [10–13], is dominated by their alkylation and arylation reactions with suitable electrophiles, and their reactivity as metalloligands, forming sulfide-bridged multi-metallic complexes. Despite their extensive chemistry, new pathways of reactivity continue to be developed, such as in the reactivity towards a chloropyridinium salt and $NH_3$, resulting in the formation of the novel binuclear platinum μ-amido complex $[Pt_2(\mu\text{-}S)(\mu\text{-}NH_2)(PPh_3)_4]^+$ [14].



1; E = S
2; E = Se

3

4
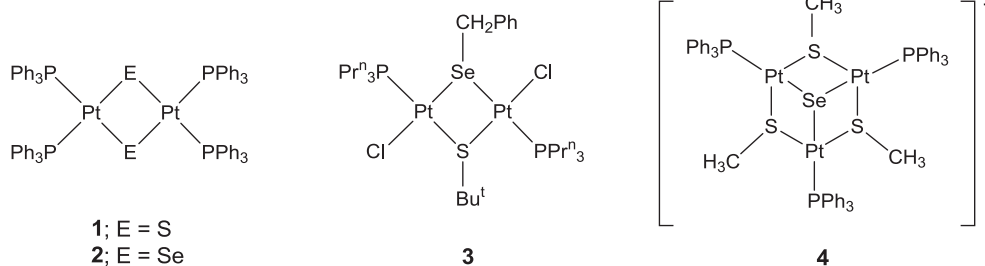
* Corresponding author.
  E-mail address: w.henderson@waikato.ac.nz (W. Henderson).

There are only two reported complexes in the literature that contain the {Pt(μ-S)(μ-Se)Pt} mixed-chalcogenide core, these being the binuclear complex [(L)ClPt(μ-S$^t$Bu)(μ-SeCH$_2$Ph)PtCl(L)] (L = PPr$_3^n$) **3** [15] and the trinuclear μ$_3$-selenido complex [(PtPPh$_3$)$_3$ (μ$_2$-SMe)$_3$(μ$_3$-Se)]$^+$ **4** [16]. Accordingly, we were interested in exploring routes to unknown, mixed-chalcogenide complexes of the general type [Pt$_2$(μ-E$_1$)(μ-E$_2$)(PPh$_3$)$_4$] where E$_1$ ≠ E$_2$ = S, Se, Te and typified by [Pt$_2$(μ-S)(μ-Se)(PPh$_3$)$_4$] **5a**. The methodology used exploits the efficacy of electrospray ionisation mass spectrometry (ESI MS) [17] as a rapid, efficient and informative technique for exploring the chemistry of these metal chalcogenide systems [11], and in this contribution we describe a detailed ESI MS investigation of such mixed-chalcogenide systems.



**5a**
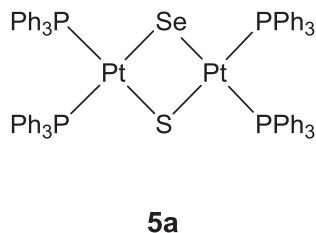
## 2. Results and discussion

### 2.1. Exchange reaction of [Pt$_2$(μ-S)$_2$(PPh$_3$)$_4$] and [Pt$_2$(μ-Se)$_2$(PPh$_3$)$_4$] in ethanol

Initially, exchange of the chalcogenide ligands between complexes [Pt$_2$(μ-S)$_2$(PPh$_3$)$_4$] **1** and [Pt$_2$(μ-Se)$_2$(PPh$_3$)$_4$] **2** was explored as a potential route to the complex [Pt$_2$(μ-S)(μ-Se)(PPh$_3$)$_4$] **5a**. A suspension of **1** and **2** in ethanol was stirred at room temperature for 12 h, with the initially cloudy brown suspension changing colour to orange, which was subsequently analysed by ESI MS. The mass spectrum contains two main peaks, with the base peak of the spectrum at m/z 1503.24 assigned as combination of the protonated [**1** + H]$^+$ and oxidised [**1**]$^+$ ions, as detailed in the literature [11]. An isotope pattern comparison of the [M]$^+$/[M + H]$^+$ ions of **1**, involving a calculated pattern (generated using the software mMass [18]) was consistent with a 1:1 combination of [M]$^+$ and [M + H]$^+$ ions. The second peak at m/z 1598.12 is assigned as the oxidised [**2**]$^+$ ion, with no evidence of the protonated [**2** + H]$^+$ ion. The observation of these ions is consistent with an incomplete reaction, possibly due in part to the limited solubility of both **1** and **2** in alcohols.

An ion observed at m/z 1550.18 is assigned as the desired mixed-chalcogenide ion [Pt$_2$(μ-S)(μ-Se)(PPh$_3$)$_4$]$^+$ (**5a**$^+$) observed in its oxidised form (calculated m/z 1550.18). The apparent proclivity for oxidation observed in the parent selenide **2** and mixed-chalcogenide **3** complexes suggests that the oxidation of the μ-selenide ligand may be preferred over protonation of the μ-sulfide in [Pt$_2$(μ-S)(μ-Se)(PPh$_3$)$_4$] **5a**. [Pt$_2$(μ-S)(μ-OH)(PPh$_3$)$_4$]$^+$ (calculated m/z 1487.27) was observed as a low intensity ion. This μ-hydroxo species has been identified previously, but not structurally characterised [14]. There are also several minor but noteworthy lower-mass ions; an ion at m/z 719.15 is assigned as a combination of the known cyclometallated ion [(Ph$_3$P)Pt(Ph$_2$PC$_6$H$_4$)]$^+$ [19] and the known hydride [(Ph$_3$P)$_2$PtH]$^+$ [20], combined in a ratio of 2:3 respectively based on comparison with an isotope pattern modelled using mMass software [18]. An ion at m/z 751.13 has an isotope pattern indicating an overlay of [M]$^+$ and [2M]$^{2+}$ ions, and is assigned as a combination of [Pt(PPh$_3$)$_2$S]$^+$ and the doubly-oxidised

[**1**]$^{2+}$ with a calculated isotope pattern agreeing closely with the experimentally-observed pattern. The parent selenide complex **2** is responsible for an analogous peak at m/z 799.07, with a combination of [Pt(PPh$_3$)$_2$Se]$^+$ and [**2**]$^{2+}$ ions making up an experimentally observed pattern that also agrees closely with the calculated pattern.

The remaining low-mass ions are all related to the mononuclear ion [(Ph$_3$P)$_2$PtSe$_2$]$^+$, which is observed at m/z 877.98 (calculated m/z 877.98) and has a distinctive isotope pattern agreeing closely with its calculated pattern. The related ions are (for [M] = [(Ph$_3$P)$_2$PtSe$_2$]) [M + OH]$^+$ at m/z 894.98 (calculated m/z 894.98), [M + ONa]$^+$ at m/z 916.97 (calculated m/z 916.97), and [M + SNa]$^+$ at m/z 932.94 (calculated m/z 932.94). Of the several higher mass (ca. m/z 2000) ions, three are all related as μ$_3$-E trimetallic aggregates with a [PtH (PPh$_3$)]$^+$ fragment, tentatively assigned as [Pt$_2$(μ$_3$-S)$_2$(PPh$_3$)$_4$PtH (PPh$_3$)]$^+$ at m/z 1961.29 (calculated m/z 1961.30), [Pt$_2$(μ$_3$-S)(μ$_3$-Se) (PPh$_3$)$_4$PtH(PPh$_3$)]$^+$ at m/z 2008.24 (calculated m/z 2008.25), and [Pt$_2$(μ$_3$-Se)$_2$(PPh$_3$)$_4$PtH(PPh$_3$)]$^+$ at m/z 2055.18 (calculated m/z 2055.19). The coordination of **1** as a metalloligand towards a platinum(II) hydride fragment has been described in the literature [21], with the complex [Pt$_2$(μ$_3$-S)$_2$(PPh$_3$)$_4$PtH(PPh$_3$)]PF$_6$ being structurally characterised by $^{31}$P{$^1$H} NMR and single-crystal X-ray diffraction.

### 2.2. Reactivity of [Pt$_2$(μ-E)$_2$(PPh$_3$)$_4$] towards elemental chalcogens

In the hope of obtaining a cleaner synthetic route to the mixed chalcogenide species [Pt$_2$(μ-S)(μ-Se)(PPh$_3$)$_4$] **5a**, the reactions of **2** with S$_8$, and of **1** with grey selenium were attempted. The behaviour of S$_8$ as a mild oxidising agent is known in organic reactions [22] and has been found to be more oxidising than elemental selenium, with S$_8$ having a more positive standard redox potential [23]. Therefore, the reaction of Se with [Pt$_2$(μ-S)$_2$(PPh$_3$)$_4$] **1** was not expected to proceed readily.

[Pt$_2$(μ-Se)$_2$(PPh$_3$)$_4$] **2** was reacted with a molar equivalent of S$_8$ in a mixed toluene-methanol solvent mixture. The initially cloudy brown suspension transformed to a clear dark red-brown solution after 2 h of mixing at room temperature, at which point the mass spectrum was acquired, and found to show two dominant ions at m/z 1551.22 and 1503.28. The generation of the mixed-chalcogenide {Pt$_2$SSe} species **5a** is immediately evident by the ion at m/z 1551.22 with a moderate relative intensity. Examination of the isotope pattern indicated a combination of protonated [**5a** + H]$^+$ and mono-oxidised [**5a**]$^+$ ions in a ratio of approximately 1:1, modelled using mMass software [18]. The protonated parent selenide complex [**2** + H]$^+$, observed at m/z 1599.16 (calculated m/z 1599.14), and sulfide complex [**1** + H]$^+$, observed at m/z 1503.28 (calculated m/z 1503.25), displayed isotope patterns absent of any contribution from their respective oxidised [M]$^+$ ions.

**Table 1**

| n | Chalcogen composition | m/z | |
| --- | --- | --- | --- |
| | | Observed | Calculated |
| 1 | {SeS$_2$} | 2040.25 | 2040.22 |
| | {Se$_2$S} | 2088.18 | 2088.17 |
| | {Se$_3$} | 2135.13 | 2135.11 |
| 2 | {SeS$_3$} | 2072.21 | 2072.19 |
| | {Se$_2$S$_2$} | 2120.15 | 2120.14 |
| | {Se$_3$S} | 2167.11 | 2167.08 |
| | {Se$_4$} | 2214.05 | 2214.03 |
| 3 | {Se$_2$S$_3$} | 2152.12 | 2152.11 |
| | {Se$_3$S$_2$} | 2199.08 | 2199.05 |

A grouping of high mass (*ca. m/z* 2100) monocations is tentatively assigned as trimetallic derivatives of the structure $[Pt_3(\mu_3\text{-E})_2(PPh_3)_5E_nH]^+$ **6** (n = 1–3; E = S, Se) whose observed and calculated *m/z* values are summarised in Table 1. The location of the chalcogenides cannot be ascertained by ESI MS, so the $\mu_3$-E ligands and $E_nH$ ligand are interchangeable for E with many isomers possible.



**6**; E = S, Se
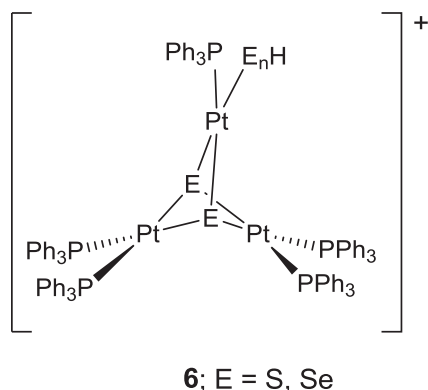
In contrast, the reaction of $[Pt_2(\mu\text{-S})_2(PPh_3)_4]$ with a large excess of Se in ethanol for 48 h, followed by filtration of the reaction solution and analysis by ESI MS showed little reaction. This was not unexpected since elemental selenium is a poorer oxidant compared to $S_8$. Absent from the spectrum were any ions related to $[Pt_2(\mu\text{-Se})_2(PPh_3)_4]$ **2** in the form of $[\mathbf{2}]^+$, $[\mathbf{2} + H]^+$, or $[\mathbf{2}]^{2+}$. A prominent base peak at *m/z* 1503.07 was assigned as a combination of oxidised $[\mathbf{1}]^+$ and protonated $[\mathbf{1} + H]^+$ ions in an approximate 1:1 ratio. Of medium relative intensity is a peak at *m/z* 1519.06, also assigned as a combinatorial isotope pattern, containing the ions $[Pt_2(\mu\text{-S})(\mu\text{-SO})(PPh_3)_4]^+$ and its protonated $[M + H]^+$ analogue in a 1:1 ratio. The calculated isotope pattern of this combination agreed closely with the observed pattern. At low relative intensities are ions *m/z* 1535.05, assigned as the known [24] S—O—H—O—S bridged di-oxidised species $[Pt_2(\mu\text{-S}_2O_2H)(PPh_3)_4]^+$ (calculated *m/z* 1535.24), and *m/z* 1551.03 assigned as the protonated mixed-chalcogenide ion $[\mathbf{5a} + H]^+$ (calculated *m/z* 1551.19). Other noteworthy ions are *m/z* 579.12 (assigned as the triphenylphosphine oxide sodium adduct $[(Ph_3PO)_2Na]^+$, calculated *m/z* 579.16, and formed by aerial oxidation of displaced $PPh_3$), *m/z* 806.01 (assigned as the mononuclear species $[(Ph_3P)_2PtS_2]Na^+$, calculated *m/z* 806.08), and *m/z* 853.97 (assigned as the analogous $[(Ph_3P)_2PtSeS]Na^+$, calculated *m/z* 854.03).

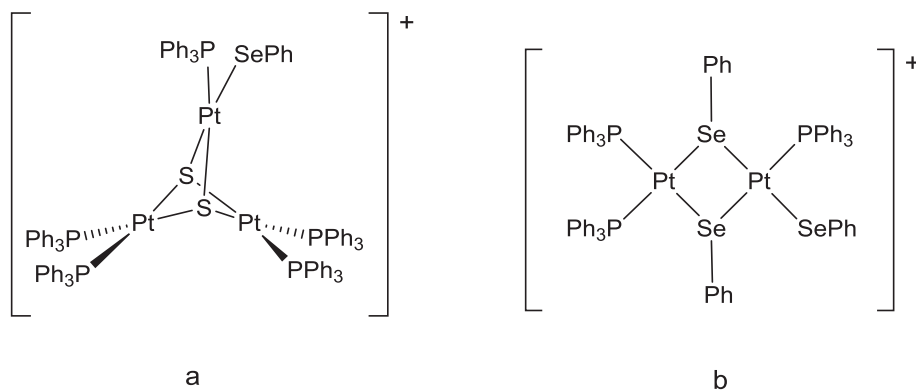### 2.3. Reactivity of $[Pt_2(\mu\text{-E})_2(PPh_3)_4]$ (E = S, Se) towards diphenyl dichalcogenides $Ph_2E_2$ (E = S, Se)

As the preceding reactions had limited success in generating the mixed-core {$Pt_2SeS$} species, microscale reactions of complexes $[Pt_2(\mu\text{-S})_2(PPh_3)_4]$ **1** and $[Pt_2(\mu\text{-Se})_2(PPh_3)_4]$ **2** with diaryl dichalcogenides, $Ph_2Se_2$ and $Ph_2S_2$, respectively, were carried out with the intention of synthesising a phenylated mixed-chalcogenide species with the {$Pt_2E_1E_2Ph$} core. Previously, we have reported that the reaction of $[Pt_2(\mu\text{-S})_2(PPh_3)_4]$ with $Ph_2S_2$ results in the formation of the mixed sulfide-thiophenolate complex $[Pt_2(\mu\text{-S})(\mu\text{-SPh})(PPh_3)_4]^+$ [25] and the commercial availability of $Ph_2Se_2$ (and $Ph_2Te_2$, *vide infra*) suggested that this could be a more promising route.

Reaction of $[Pt_2(\mu\text{-S})_2(PPh_3)_4]$ with $Ph_2Se_2$ was carried out in methanol suspension at room temperature for 24 h before filtering

to remove insoluble matter, resulting in a clear yellow solution. Reaction progress was monitored with positive-ion ESI MS and a time series of spectra can be seen in Fig. 1. After 30 min. the mass spectrum showed two significant peaks. The main peak at *m/z* 1503.39 is assigned to $[\mathbf{1}]^+$ and $[\mathbf{1} + H]^+$, and a lesser peak at *m/z* 1659.35 assigned to the phenylselenium addition ion $[Pt_2(\mu\text{-S})(\mu\text{-SSePh})(PPh_3)_4]^+$ **7** (calculated *m/z* 1659.20) which had an isotope pattern in close agreement with the calculated pattern. The proposed structure of this species is assumed to retain the {$Pt_2S_2$} core, as the alternative phenylsulfur complex $[Pt_2(\mu\text{-Se})(\mu\text{-SSPh})(PPh_3)_4]^+$ (indistinguishable by isotope pattern) would require the dissociation of a relatively strong C—S bond. In theoretical examinations, diphenyl dichalcogenides were found to have stronger C—E bonds (C—S 291.83 kJ mol$^{-1}$, C—Se 269.62 kJ mol$^{-1}$) than E—E bonds (S—S 191 kJ mol$^{-1}$, Se—Se 182.55 kJ mol$^{-1}$) attributed to $\pi$-$\pi$ overlap between the $\pi$ orbital of the chalcogen atom and adjacent phenyl carbon, resulting in a strengthened C—E bond [26]. Experimental observations agree with the calculated bond strengths, with C—S bonds (300.14 kJ mol$^{-1}$) found to be stronger than S—S bonds (192 kJ mol$^{-1}$) which in turn are stronger than Se—Se bonds (172 kJ mol$^{-1}$); no experimental data could be located in the literature for C—Se bond dissociation of diphenyl diselenide [27,28]



**7**
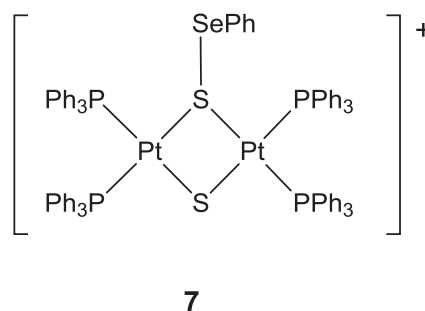
The spectrum included various ions at very low relative intensities (*ca.* 2.5%) which were tentatively assigned by their isotope pattern and *m/z* value. Of note are mononuclear ions at *m/z* 718.22, assigned to the known cyclometallated species $[Pt(PPh_3)(PPh_2C_6H_4)]^+$ (calculated *m/z* 718.14) [19], *m/z* 784.18, assigned as an overlapping of the oxidised ion $[Pt(PPh_3)_2S_2]^+$ (calculated *m/z* 783.09) and the protonated ion $[Pt(PPh_3)_2SSH]^+$ (calculated *m/z* 784.10), and *m/z* 876.19 assigned as the previously-observed phenylselenolate ion $[Pt(PPh_3)_2SePh]^+$ (calculated *m/z* 876.10). A common fragment ion observed when employing a moderate capillary exit voltage involves loss of a neutral triphenylphosphine; a fragment ion of this type is observed at *m/z* 1397.23, and is assigned as $[Pt_2(\mu\text{-S})(\mu\text{-SSePh})(PPh_3)_3]^+$ (calculated *m/z* 1397.10). A low intensity ion at *m/z* 1627.37 was assigned to the mixed chalcogenide arylated cation $[Pt_2(\mu\text{-S})(\mu\text{-SePh})(PPh_3)_4]^+$ (**8**, calculated *m/z* 1627.22) which has an isotope pattern agreeing closely with the calculated pattern. Similar to the phenylselenium addition ion **7**, the structure is assumed based on the difficulty of dissociating the Se-$C_{Ph}$ bond; $[Pt_2(\mu\text{-Se})(\mu\text{-SPh})(PPh_3)_4]^+$ **9** would be indistinguishable by ESI MS as it is isobaric. The presence in the spectrum of the mononuclear phenylselenolate ion $[Pt(SePh)(PPh_3)_2]^+$ (*m/z* 876.10), possibly from the fragmentation of **8**, and absence of the phenylthiolate analogue $[Pt(SPh)(PPh_3)_2]^+$, strongly suggests the presence of a bridging phenylselenolate ligand *viz.* $[Pt_2(\mu\text{-S})(\mu\text{-SePh})(PPh_3)_4]^+$ **8**.

**8**         **9**         **10**

Re-analysis of the reaction mixture after 24 h produced a spectrum (Fig. 1b) with some notable changes. The base peak was now the ion $[Pt_2(\mu\text{-}S)(\mu\text{-}SSePh)(PPh_3)_4]^+$ **7** at $m/z$ 1659.19, while a peak of moderate intensity at $m/z$ 1517.25 was assigned as the methylated species $[Pt_2(\mu\text{-}S)(\mu\text{-}SMe)(PPh_3)_4]^+$ (calculated $m/z$ 1517.26) which has been observed previously when $[Pt_2(\mu\text{-}S)_2(PPh_3)_4]$ **1** is reacted in methanol [25]. A low intensity ion at $m/z$ 1873.00 had an isotope pattern indicating a monocation of multiple polyisotopic elements; this ion was subsequently assigned as the trimetallic aggregate **10**, following investigations of the reactivity of $[Pt_2(\mu\text{-}E)_2(PPh_3)_4]$ (E = S, Se) with diaryl ditellurides (*vide infra*).

After 72 h some significant changes in occurred in the ESI mass spectrum (Fig. 1c): the methylated complex $[Pt_2(\mu\text{-}S)(\mu\text{-}SMe)(PPh_3)_4]^+$ ($m/z$ 1517.28) increased in relative intensity, becoming the base peak of the spectrum, while the protonated parent complex $[\mathbf{1}+H]^+$ was no longer present. The relative intensity of the peaks at $m/z$ 1627.25 (**8**) and $m/z$ 1873.03 increased significantly, while a

new peak at $m/z$ 2117.27 was observed and assigned as the trinuclear aggregate $[Pt_3(\mu_3\text{-}S)_2(PPh_3)_5(SePh)]^+$ (calculated $m/z$ 2117.25) with a proposed structure shown in Scheme 1a. After two weeks, the ESI mass spectrum (Fig. 1d) showed a base peak at $m/z$ 579.18 due to $[(Ph_3PO)_2Na]^+$. Ions pertaining to the mixed-chalcogenide arylated species **8** at $m/z$ 1627.28 and the phenylselenium addition ion **7** at $m/z$ 1659.26 were observed at very low relative intensities. A low intensity ion at $m/z$ 1645.13 was assigned as a tri-phenylselenolate, $PPh_3$-displaced complex $[Pt_2(\mu\text{-}SePh)_2(PPh_3)_3(SePh)]^+$ (calculated $m/z$ 1645.07) with a proposed structure displayed in Scheme 1b.

The corresponding microscale reaction of $[Pt_2(\mu\text{-}Se)_2(PPh_3)_4]$ **2** and diphenyl disulfide ($Ph_2S_2$) in methanol for 24 h gave a cloudy dark-red suspension. Filtration to remove insoluble matter gave a clear dark-red filtrate which was analysed by positive-ion ESI MS. The base peak at $m/z$ 1627.19 is assigned to the mixed-chalcogenide species $[Pt_2(\mu\text{-}Se)(\mu\text{-}SPh)(PPh_3)_4]^+$ (**9**, calculated $m/z$ 1627.22) which is tentatively assigned as the $\mu$-phenylthiolato



**Fig. 1.** A time series of mass spectra for the reaction of $[Pt_2(\mu\text{-}S)_2(PPh_3)_4]$ **1** and $Ph_2Se_2$ in methanol after (a) 30 min, (b) 24 h, (c) 72 h and (d) two weeks.

**Scheme 1.** Proposed structures of (a) the trinuclear aggregate $[Pt_3(\mu_3-S)_2(PPh_3)_5(SePh)]^+$ (calculated $m/z$ 2117.25) and (b) the diarylated binuclear PPh$_3$-displaced $[Pt_2(\mu-SePh)_2(PPh_3)_3(SePh)]^+$ ion (calculated $m/z$ 1645.07).

complex and is thus an isomer of the μ-phenylselenolato complex **8** (*vide supra*).

An ion at $m/z$ 1613.12 is assigned as the methylselenolate complex $[Pt_2(\mu-Se)(\mu-SeMe)(PPh_3)_4]^+$ (calculated $m/z$ 1613.15) and mirrors the previous reaction with **1** and Ph$_2$Se$_2$ (*vide supra*) in which methanol promoted methylation. Some other key differences from the analogous reaction of $[Pt_2(\mu-S)_2(PPh_3)_4]$ **1** and Ph$_2$Se$_2$ in methanol are: (i) the prominence of high-mass peaks at $m/z$ 2164.14 and $m/z$ 2243.06, attributed to the trimetallic aggregate species $[Pt_2(\mu-Se)_2(PPh_3)_4Pt(PPh_3)(R)]^+$ where R = SPh (calculated $m/z$ 2164.20) and R = SeSPh (calculated $m/z$ 2243.11), with proposed structures as shown in Scheme 2; (ii) a very weak ion at $m/z$ 1707.10 for the phenylsulfur addition complex (tentatively assigned as $[Pt_2(\mu-Se)(\mu-SeSPh)(PPh_3)_4]^+$ **11**, calculated $m/z$ 1707.14), and (iii) no ion observed for either of the mononuclear species $[Pt(SePh)(PPh_3)_2]^+$ (calculated $m/z$ 875.10) or $[Pt(SPh)(PPh_3)_2]^+$ (calculated $m/z$ 828.16).



**11**
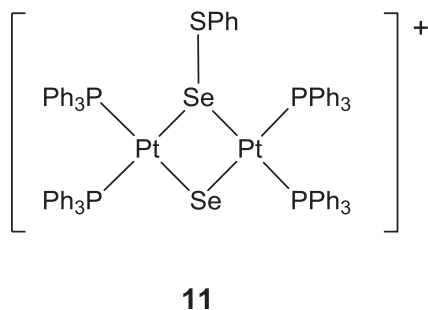
In order to avoid alkylation by methanol, the microscale reaction of $[Pt_2(\mu-Se)_2(PPh_3)_4]$ **2** and Ph$_2$S$_2$ was repeated in ethanol and the brown suspension analysed by ESI MS after 24 and 48 h (Fig. 2). After 24 h the mass spectrum (Fig. 2a) showed similar features to the analogous reaction in methanol, *sans* the methylated selenide ion $[Pt_2(\mu-Se)(\mu-SeMe)(PPh_3)_4]^+$ at $m/z$ 1613 and also no evidence of the ethylated ion $[Pt_2(\mu-Se)(\mu-SeEt)(PPh_3)_4]^+$. The ion of highest intensity is the mixed-chalcogenide species $[Pt_2(\mu-Se)(\mu-SPh)(PPh_3)_4]^+$ **9**. Ethanol appears to be poorer than methanol at solubilising the parent selenide complex $[Pt_2(\mu-Se)_2(PPh_3)_4]$ **2**, with a peak of moderate intensity observed at $m/z$ 1598.13 assigned as $[2]^+$. At a similar intensity to the oxidised $[2]^+$ ion is the phenylsulfur addition ion $[Pt_2(\mu-Se)(\mu-SeSPh)(PPh_3)_4]^+$ (**11**, $m/z$ 1707.15); notably this species was almost undetectable in the previous reaction in methanol (∼1% relative intensity). After 48 h (Fig. 2b) the base peak is the phenylthiolato complex **9** ($m/z$ 1627.29) as before, with the disappearance of ions $[2]^+$ at $m/z$ 1598 and **11** at $m/z$ 1707. Significant ions at $m/z$ 2163.28 and $m/z$

2243.20 indicate the formation of trinuclear aggregates (Scheme 2) with the resulting displacement and oxidation of PPh$_3$ effecting the observation of the adduct ion $[(Ph_3PO)_2Na]^+$ ($m/z$ 579.20). When the microscale reaction of $[Pt_2(\mu-S)_2(PPh_3)_4]$ **1** and Ph$_2$Se$_2$ was also carried out replacing the methanol solvent by ethanol the outcome was largely the same, bar the absence of the methylated species $[Pt_2(\mu-S)(\mu-SMe)(PPh_3)_4]^+$.

The reaction of Ph$_2$Se$_2$ and **1** (reaction **A**) proceeds more slowly than the corresponding reaction of Ph$_2$S$_2$ and **2** (reaction **B**), reflected in the longevity of starting complex **1** and quickly disappearing **2** (detected as protonated $[M + H]^+$ or oxidised $[M]^+$ cations) in the ESI mass spectra. This difference is presumably related to the greater oxidising ability of Ph$_2$S$_2$ compared to Ph$_2$Se$_2$. Another observable difference was the longevity in the reaction solution of the phenylselenium addition ion $[Pt_2(\mu-S)(\mu-SSePh)(PPh_3)_4]^+$ **7** in reaction **A** *cf.* the relatively short-lived phenylsulfur analogue $[Pt_2(\mu-Se)(\mu-SeSPh)(PPh_3)_4]^+$ **11** in reaction **B**.

### 2.4. Reactivity of $[Pt_2(\mu-E)_2(PPh_3)_4]$ (E = S, Se) towards diaryl ditellurides R$_2$Te$_2$

The success in identifying mixed-chalcogenide complexes $[Pt_2(\mu-S)(\mu-SePh)(PPh_3)_4]^+$ **8** and $[Pt_2(\mu-Se)(\mu-SPh)(PPh_3)_4]^+$ **9** using diphenyl dichalcogenides (*vide supra*) suggested that the extension to tellurium chemistry should also be productive in the generation of complexes with mixed {Pt$_2$STe} and {Pt$_2$SeTe} cores.

The reaction of $[Pt_2(\mu-Se)_2(PPh_3)_4]$ **2** and Ph$_2$Te$_2$ in ethanol was initially carried out on a microscale with the light-brown suspension stirred at room temperature for 48 h, resulting in a dark-red solution. The progress of the reaction was monitored *via* ESI MS at 12, 24 and 48 h, and a time series of mass spectra is shown in
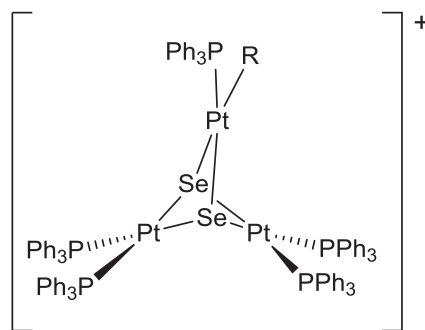


**Scheme 2.** The proposed structure of trimetallic aggregates $[Pt_2(\mu-Se)_2(PPh_3)_4Pt(PPh_3)(R)]^+$ where (a) R = SPh (calculated $m/z$ 2164.20) and (b) R = SeSPh (calculated $m/z$ 2243.11).
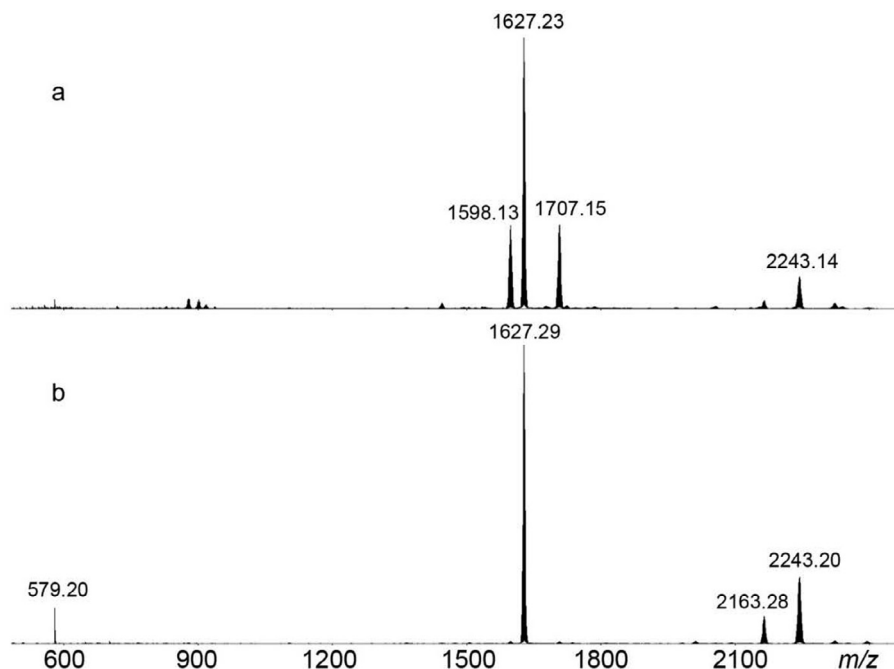
**Fig. 2.** The positive-ion ESI mass spectra of a mixture of [Pt₂(μ-Se)₂(PPh₃)₄] **2** and Ph₂S₂ in ethanol after (a) 24 h and (b) 48 h.

Fig. 3. The ESI mass spectrum after 12 h (Fig. 3a) has three main peaks with the dominant base peak at $m/z$ 1002.99 assigned as the mononuclear ion $[Pt(PPh_3)_2SeTePh]^+$ (calculated $m/z$ 1003.1), with an observed isotope pattern agreeing closely with the calculated pattern. Of the two lower intensity ions, that at $m/z$ 1803.03 was identified as the phenyltellurium addition ion $[Pt_2(\mu\text{-Se})(\mu\text{-SeTePh})(PPh_3)_4]^+$ (**12**, calculated $m/z$ 1803.07). The other ion at $m/z$ 2065.87 was identified as a large cation with an isotope pattern indicating a 1+ charge and a composition of polyisotopic elements. Following a series of other experiments (*vide infra*), this ion was assigned as the trinuclear complex [{Pt(PPh₃)}₃(μ₃-Se)(μ-TePh)₃]⁺ **13b** (see Scheme 3). A comparison of the calculated and experimental isotope patterns of [{Pt(PPh₃)}₃(μ₃-Se)(μ-TePh)₃]⁺ **13b** is shown in Fig. 4. Although related complexes with μ-thiolate ligands have been reported (*vide infra*) [16], analogues with μ-tellurolates are hitherto unknown.

$(PPh_3)_4]^+$ at $m/z$ 1803, and the isomer of **14**, *viz.* $[Pt_2(\mu\text{-Te})(\mu\text{-SePh})(PPh_3)_4]^+$ at $m/z$ 1723, cannot be structurally dismissed, but would require the transfer of a phenyl group. The Te—C bond, although shown to be weaker than E–C bonds of the lighter chalcogenides [28], would still be of significant strength due to the phenyl-tellurium π orbital interaction decreasing the likelihood of dissociation.

The microscale reaction was re-examined by ESI MS after 24 h, revealing a much cleaner spectrum (Fig. 3b) with the trinuclear cation [{Pt(PPh₃)}₃(μ₃-Se)(μ-TePh)₃]⁺ **13b** at $m/z$ 2065.93 being the base peak. The ion $[Pt(PPh_3)_2SeTePh]^+$ at $m/z$ 1003.01 had significantly decreased in intensity. After 48 h the reaction mixture was analysed by ESI MS for a final time (Fig. 3c) and found to consist of only [{Pt(PPh₃)}₃(μ₃-Se)(μ-TePh)₃]⁺ **13b**. This ion shows appreciable stability towards fragmentation, with a sample analysed using a (very high) capillary exit voltage of 300 V still showing **13b** as the base peak.



**12**



**14**
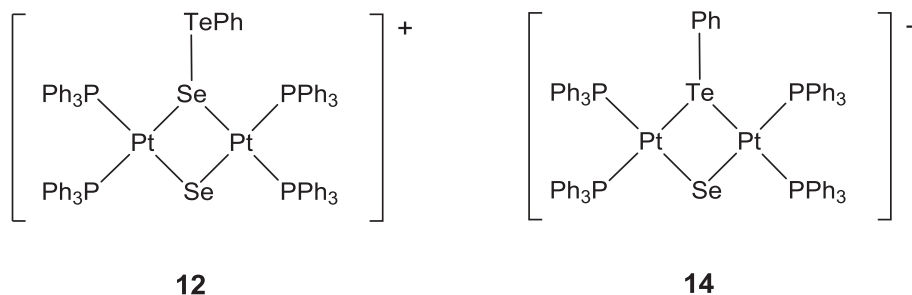
An ion of low intensity at $m/z$ 1540.95, assigned as $[Pt_2(\mu\text{-Se})(\mu\text{-SeTePh})(PPh_3)_3]^+$ (calculated $m/z$ 1540.98), appears to be a product of fragmentation *via* PPh₃ loss from **12**. The mono-oxidised ion **[2]⁺** appears at low relative intensity ($m/z$ 1598.09) as does the arylated mixed-chalcogenide core {Pt₂SeTe} ion $[Pt_2(\mu\text{-Se})(\mu\text{-TePh})(PPh_3)_4]^+$ **14** at $m/z$ 1723.12 (calculated $m/z$ 1723.16). It must again be noted that the isomer of **12**, *viz.* $[Pt_2(\mu\text{-Te})(\mu\text{-SeSePh})$

Evidence for the constitution of the trinuclear cation [{Pt(PPh₃)}₃(μ₃-Se)(μ-TePh)₃]⁺ **13b** was obtained by additional mass spectrometry experiments, in addition to unequivocal characterisation by X-ray crystallography (*vide infra*). When [Pt₂(μ-Se)₂(PPh₃)₄] **2** was reacted in ethanol with a substituted derivative of diphenyl ditelluride *viz.* (p-EtOC₆H₄)₂Te₂, a dark-red solution was obtained, which was examined by ESI MS. The mass spectrum

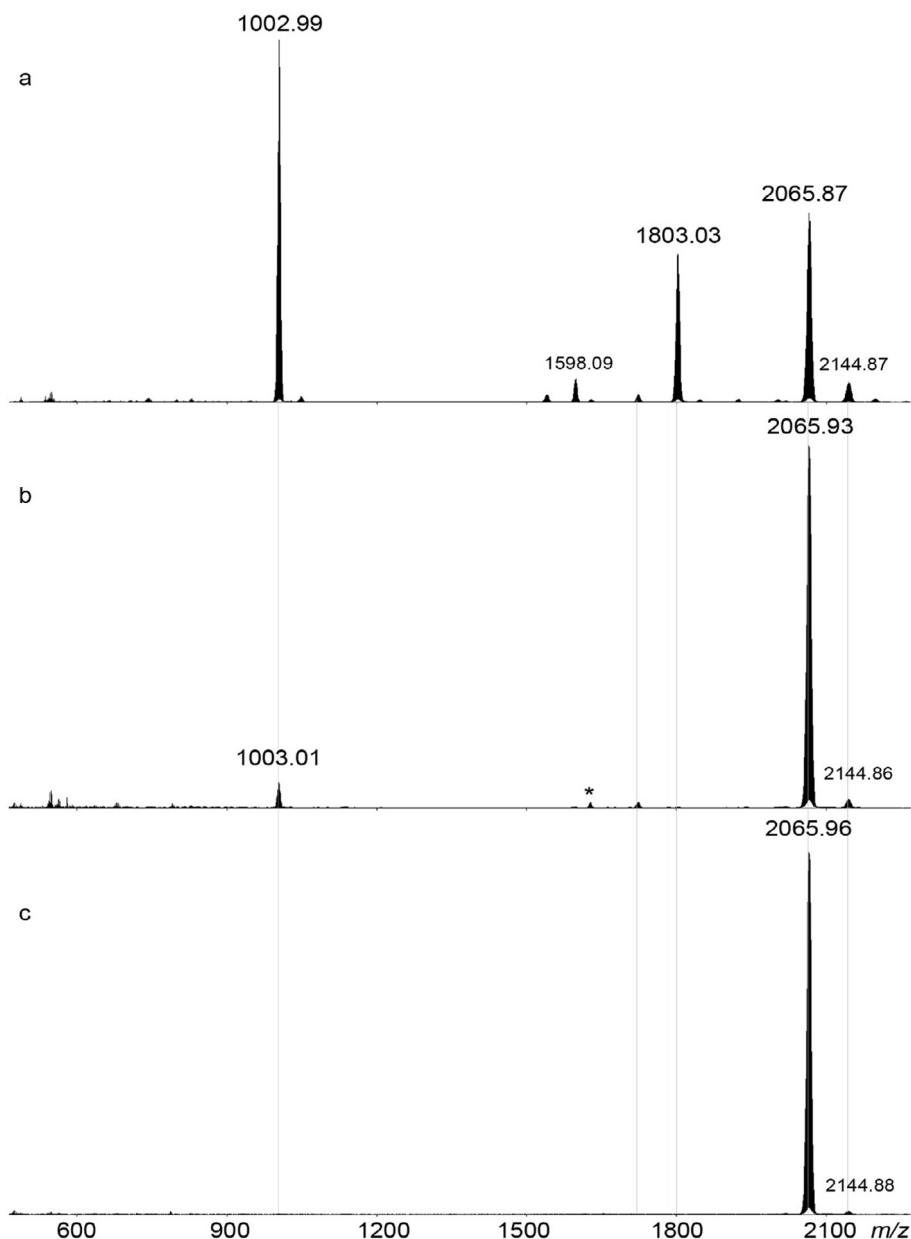**Fig. 3.** Time series of positive-ion ESI mass spectra of $[Pt_2(\mu\text{-}Se)_2(PPh_3)_4]$ **2** and $Ph_2Te_2$ in ethanol with spectra acquired after (a) 12 h, (b) 24 h and (c) 48 h. (* = residual ion from preceding analyte).

(Fig. 5) was very similar in appearance to spectra obtained from the reaction of $[Pt_2(\mu\text{-}Se)_2(PPh_3)_4]$ **2** and $Ph_2Te_2$ in ethanol. The monocationic base peak of the spectrum at $m/z$ 2197.94, assigned as **13c**, was sandwiched by two peaks of low relative intensity at $m/z$ 2154.92 and $m/z$ 2275.86, the latter peak displaying an isotope pattern consistent with an overlapping of $[M]^+$ and $[2M]^{2+}$ ions. An ion at $m/z$ 1047.01 was assigned (by isotope pattern comparison) as $[Pt(PPh_3)_2SeTeC_6H_4OEt]^+$ (calculated $m/z$ 1047.04), analogous to the ion $[Pt(PPh_3)_2SeTePh]^+$ observed with $Ph_2Te_2$. Comparing this spectrum (Fig. 5) with spectra of the previous reaction between **2** and $Ph_2Te_2$ (Fig. 3), the mass difference (132 Da) between the cations at $m/z$ 2197.9 and $m/z$ 2065.9 is 3 times the mass difference (of 44 Da) between $p$-EtOC$_6$H$_4$ (127.07 Da) and phenyl (77.04 Da) groups. Considering also the probable greater dissociation energy of the Te—C$_{Ph}$ bond $cf.$ the relatively weak Te—Te bond (138 kJ mol$^{-1}$) [29], inferred from the known E-C$_{Ph}$ bond dissocia-

tion energy order (Se—C < S—C, with Se—C$_{Ph}$ 269.6 kJ mol$^{-1}$ and S—C$_{Ph}$ 291.8 kJ mol$^{-1}$) [26] and the phenyl-chalcogen $\pi$ orbital interaction in the E—C bond, it can be concluded that the complexes **13** contain three Te—Ar moieties

For additional structural identification, the reactions of the sulfide analogue $[Pt_2(\mu\text{-}S)_2(PPh_3)_4]$ **1** with both $Ph_2Te_2$ and ($p$-EtOC$_6$H$_4$)$_2$Te$_2$ were carried out. $[Pt_2(\mu\text{-}S)_2(PPh_3)_4]$ **1** and $Ph_2Te_2$ were reacted in methanol for 48 h; reaction progress was monitored by ESI MS after 30 min., 24 h and 48 h as seen in a time series of spectra in Fig. 6. Upon mixing, the red-orange suspension transformed to a clear dark-red solution after 30 min. and was promptly analysed by ESI MS (Fig. 6a). An ion at $m/z$ 1709.13 assigned as the phenyl-tellurium addition ion $[Pt_2(\mu\text{-}S)(\mu\text{-}STePh)(PPh_3)_4]^+$ (**15a**, calculated $m/z$ 1709.18) was preponderant with an isotope pattern agreeing closely with the calculated. A low intensity peak (<5% relative intensity) at $m/z$ 1677.15 was identified as the phenyltelluro-
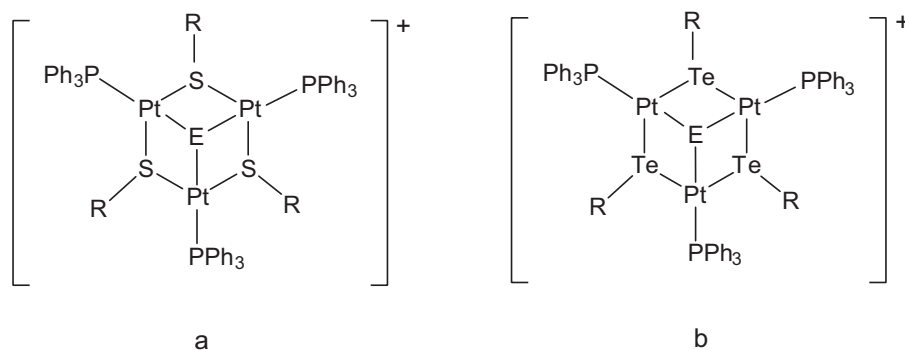
|      | E  | R           |
|------|----|-------------|
| **13a** | S  | Ph          |
| **13b** | Se | Ph          |
| **13c** | Se | $p$-C$_6$H$_4$OEt |
| **13d** | S  | $p$-C$_6$H$_4$OEt |

**Scheme 3.** A comparison of (a) complexes [{Pt(PPh$_3$)}$_3$($\mu_3$-E)($\mu$-SR)$_3$]$^+$ reported in the literature [16]; (b) proposed structures of complexes [{Pt(PPh$_3$)}$_3$($\mu_3$-E)($\mu$-TeR)$_3$]$^+$ **13a-d**
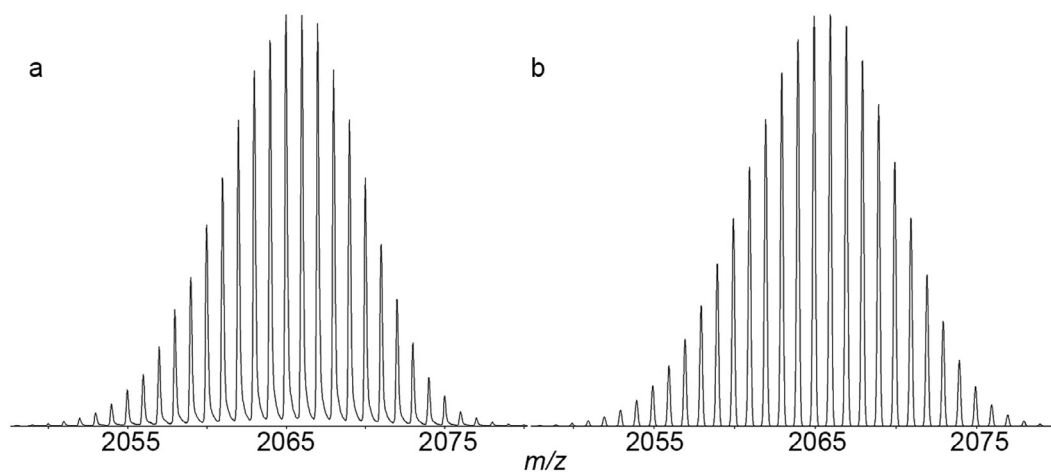


**Fig. 4.** An isotope pattern comparison for the trimetallic aggregate [{Pt(PPh$_3$)}$_3$($\mu_3$-Se)($\mu$-TePh)$_3$]$^+$ **13b**; (a) experimental ($m/z$ 2065.93) and (b) calculated ($m/z$ 2065.92).

late complex [Pt$_2$($\mu$-S)($\mu$-TePh)(PPh$_3$)$_4$]$^+$ (**16a**, calculated $m/z$ 1677.21). After 24 h the mass spectrum (Fig. 6b) showed significant changes. The base peak assigned as **15a** at $m/z$ 1709.19 was now accompanied by two medium intensity peaks. The first at $m/z$ 1677.22, was identified in the previous spectrum as **16a**. The second at $m/z$ 2018.98 was assigned as the trinuclear species [{Pt(PPh$_3$)}$_3$($\mu_3$-S)($\mu$-TePh)$_3$]$^+$ (**13a**, Scheme 3, calculated $m/z$ 2018.97). An ion of low intensity at $m/z$ 719.16 is assigned as a combination of the known cyclometallated species [(Ph$_3$P)Pt(Ph$_2$-PC$_6$H$_4$)]$^+$, and the hydride ion [(Ph$_3$P)$_2$PtH]$^+$ in approximately a 2:3 ratio respectively. Additionally, a low relative intensity mono-

cation at $m/z$ 2037.34 can be tentatively assigned as the trimetallic aggregate [Pt$_3$($\mu_3$-S)$_2$(PPh$_3$)$_5$Ph]$^+$ (calculated $m/z$ 2037.33), indicating a likely dissociation of the Te–C bond, though the location of the phenyl group, which could be on platinum or sulfur, is not known. Diphenyl ditelluride is known to undergo C–Te bond rupture, such as in the isolation of the complex [Pd$_6$Cl$_2$Te$_4$(TePh)$_2$(-PPh$_3$)$_6$]·½CH$_2$Cl$_2$ from the reaction of Pd(PPh$_3$)$_4$ with Ph$_2$Te$_2$ in CH$_2$Cl$_2$,[30] and indeed C–Te bond cleavage is quite a well-known process in general, with a number of examples in the literature [31–33], including reactions leading to the formation of Pt–C bonds [34,35].
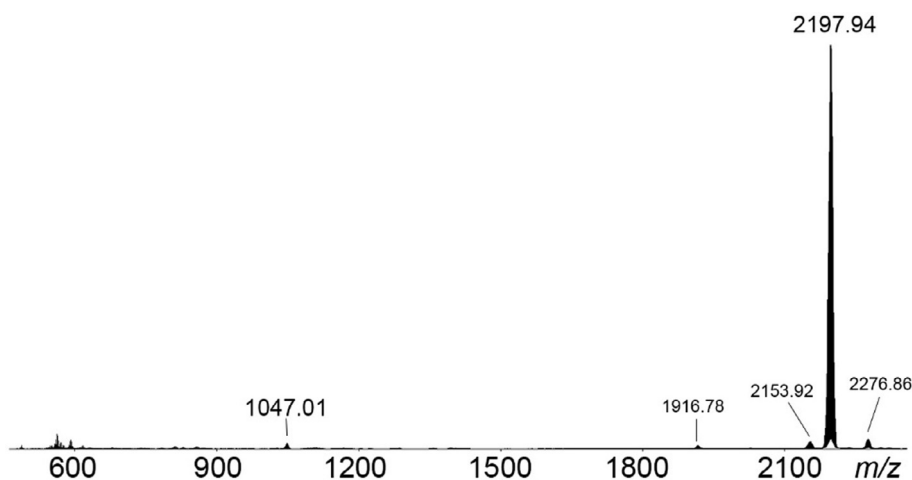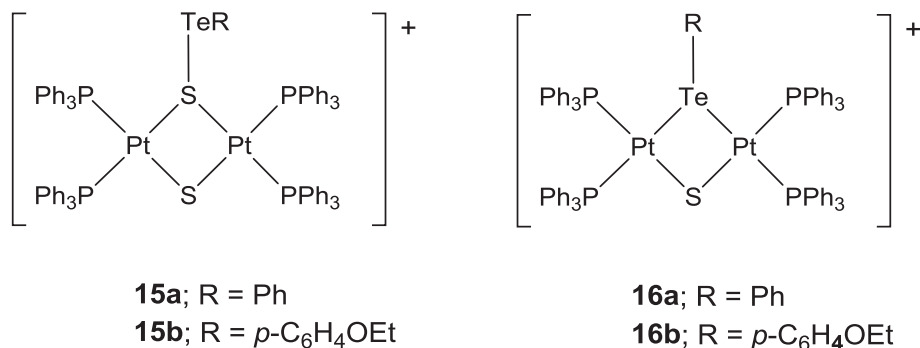
**15a**; R = Ph
**15b**; R = $p$-C$_6$H$_4$OEt

**16a**; R = Ph
**16b**; R = $p$-C$_6$H$_4$OEt



**Fig. 5.** The positive-ion ESI mass spectrum of [Pt$_2$($\mu$-Se)$_2$(PPh$_3$)$_4$] **2** and ($p$-EtOC$_6$H$_4$)$_2$Te$_2$ in ethanol after 24 h.

Comparison of the ion at $m/z$ 2066 (observed in the reaction of **2** with Ph$_2$Te$_2$) with the ion at $m/z$ 2019 observed in the analogous reaction of **1** with Ph$_2$Te$_2$ provided a mass difference of 47 Da, equivalent to the mass difference between Se (78.96 Da) and S (32.07 Da), indicating that the ions contain either one selenide (**13b**) or one sulfide (**13a**). The structures of the trinuclear cations **13a-d** are shown in Scheme 3. All experimentally-observed isotope patterns of these proposed trinuclear aggregate ions agree closely with their respective calculated isotope patterns.

Examination of the literature provides structurally similar chalcogen-containing trinuclear aggregates of Pt [16] and Pd [36] with capping $\mu_3$-chalcogenides and three $\mu$-chalcogenide ligands in a trigonal pyramidal arrangement. An investigation of platinum(II) trimetallic aggregates [{Pt(PPh$_3$)}$_3$($\mu_3$-E)($\mu$-SR)$_3$]$^+$ (E,R; S, Bn; S,Me; Se,Me) showed that out of a number of disulfides reacted with the starting mononuclear platinum(II) compound, only dibenzyl disulfide produced the trinuclear aggregate [16]. Diphenyl disulfide was found to produce a binuclear [Pt$_2$($\mu$-SPh)$_2$(PPh$_3$)$_2$Cl$_2$] species, while dialkyl disulfides quantitatively produced planar trinuclear clusters of the type [{Pt(PPh$_3$)}$_3$($\mu$-SR)$_3$]$^+$. Oxidation of these planar triplatinum clusters with chalcogens (E = S, Se) was found to be an alternative route to the trimetallic aggregates [16]. The palladium(II) trinuclear aggregate [{Pd(PPh$_3$)}$_3$($\mu_3$-Se)($\mu$-SePh)$_3$]$^+$ has a close structural resemblance to the platinum(II) aggregates, and is suggested to form *via* condensation reactions of mononuclear palladium complexes [36], a known behaviour of palladium in the synthesis of high nuclearity complexes [37].

On further analysis of the mass spectrum of [Pt$_2$($\mu$-Se)$_2$(PPh$_3$)$_4$] **2** with Ph$_2$Te$_2$ a low intensity peak at $m/z$ 2144.8 can be tentatively

assigned as [**13b** + Se]$^+$ (calculated $m/z$ 2144.84). The addition of Se could be either Se$_2^{2-}$ in place of Se$^{2-}$, or the incorporation of Se with a Te-Ph moiety as a $\mu$-SeTePh ligand, thus retaining an overall charge of +1 on the aggregate. The isotope pattern of this peak displays the properties consistent with an overlay of [M]$^+$ and [2M]$^{2+}$ ions (*vide supra*), suggesting the formation of a dimer [**13b**$_2$Se$_2$]$^{2+}$. The experimentally-observed peak at $m/z$ 2144.80 and calculated peak modelled with a 2:1 ratio of [M]$^+$ to [2M]$^{2+}$ are displayed in Fig. 7 (where [M] = **13b** + Se). Revisiting the mass spectrum acquired from the reaction of **2** with ($p$-EtOC$_6$H$_4$)$_2$Te$_2$, the assignment of a low-intensity peak at $m/z$ 2276.8 displaying an analogous overlay of [M]$^+$ and [2M]$^{2+}$ ions can be tentatively assigned in a similar fashion with [M]$^+$ = [**13c** + Se]$^+$ (calculated $m/z$ 2276.91).

Finally, the reaction of [Pt$_2$($\mu$-S)$_2$(PPh$_3$)$_4$] **1** with the substituted ditelluride ($p$-EtOC$_6$H$_4$)$_2$Te$_2$ in methanol gave a cloudy orange suspension which was reacted for 24 h at room temperature. After 1 h, the dark-red solution was examined by ESI MS producing a clean mass spectrum with the base peak at $m/z$ 1753.25 assigned as the cationic aryl-tellurium addition ion [Pt$_2$($\mu$-S){$\mu$-STeC$_6$H$_4$OEt}(PPh$_3$)$_4$]$^+$ (**15b**, calculated $m/z$ 1753.21). A lower intensity ion at $m/z$ 1721.28 was assigned as the mixed ring {Pt$_2$STe} cation [Pt$_2$($\mu$-S)($\mu$-TeC$_6$H$_4$OEt)(PPh$_3$)$_4$]$^+$ (**16b**, calculated $m/z$ 1721.24). The clear red solution was re-analysed by ESI MS after 24 h at room temperature with the less-clean mass spectrum displaying a base peak at $m/z$ 1753.19 assigned as the [Pt$_2$($\mu$-S){$\mu$-STeC$_6$H$_4$OEt}(PPh$_3$)$_4$]$^+$ addition ion **15b**. The species **16b** increased in intensity at $m/z$ 1721.22, with many lower intensity ions present. The parent complex **1** was observed at $m/z$ 751.12 as the doubly oxidised
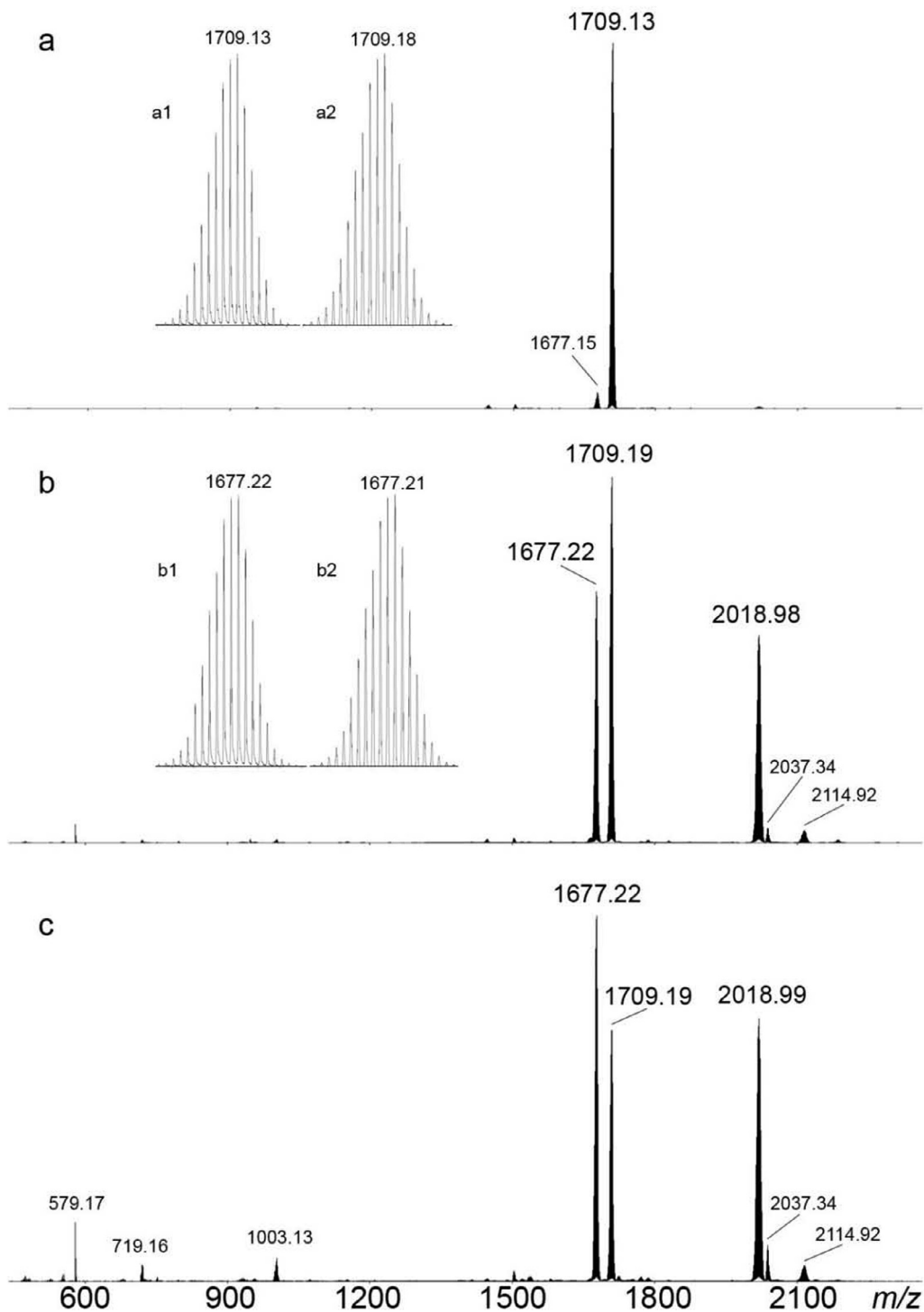
**Fig. 6.** A time series of positive-ion ESI mass spectra of the reaction of $[Pt_2(\mu\text{-S})_2(PPh_3)_4]$ **1** and $Ph_2Te_2$ in methanol after (a) 30 min, (b) 24 h and (c) 48 h. The insert in (a) is an isotope pattern comparison of (a1) the experimentally observed $m/z$ 1709.13 and (a2) the calculated $m/z$ 1709.18 for $[Pt_2(\mu\text{-S})_2(PPh_3)_4TePh]^+$ **15a**. The insert in (b) is an isotope pattern comparison of (b1) the experimentally observed $m/z$ 1677.22 and (b2) the calculated $m/z$ 1677.21 for $[Pt_2(\mu\text{-S})(\mu\text{-TePh})(PPh_3)_4]^+$ **16a**.

$[M]^{2+}$ (calculated $m/z$ 751.12) and again at $m/z$ 1503.23 as a combination of its mono-oxidised and protonated forms. The expected trimetallic aggregate $[\{Pt(PPh_3)\}_3(\mu_3\text{-S})(\mu\text{-TeC}_6H_4OEt)_3]^+$ **13d**, analogous to the aggregates **13a-c**, is detected at $m/z$ 2151.03 (calculated $m/z$ 2151.05) at a low relative intensity.

Confirmation of the identity of the products from the above reactions was achieved by a macroscopic reaction between $[Pt_2(\mu\text{-Se})_2(PPh_3)_4]$ and $Ph_2Te_2$ in ethanol solvent. The product

cation was isolated from the reaction mixture by addition of excess $NH_4PF_6$, giving $[\{Pt(PPh_3)\}_3(\mu_3\text{-Se})(\mu\text{-TePh})_3]PF_6$ as a dark-brown solid in 47% isolated yield. The complex gave satisfactory microelemental analytical and ESI MS data, and was able to be unequivocally characterised by means of an X-ray structure determination.

Crystals of the complex $[\{Pt(PPh_3)\}_3(\mu_3\text{-Se})(\mu\text{-TePh})_3]PF_6$ were obtained by recrystallisation from an acetone-hexane solution. The molecular structure of the cation is shown in Fig. 8 and
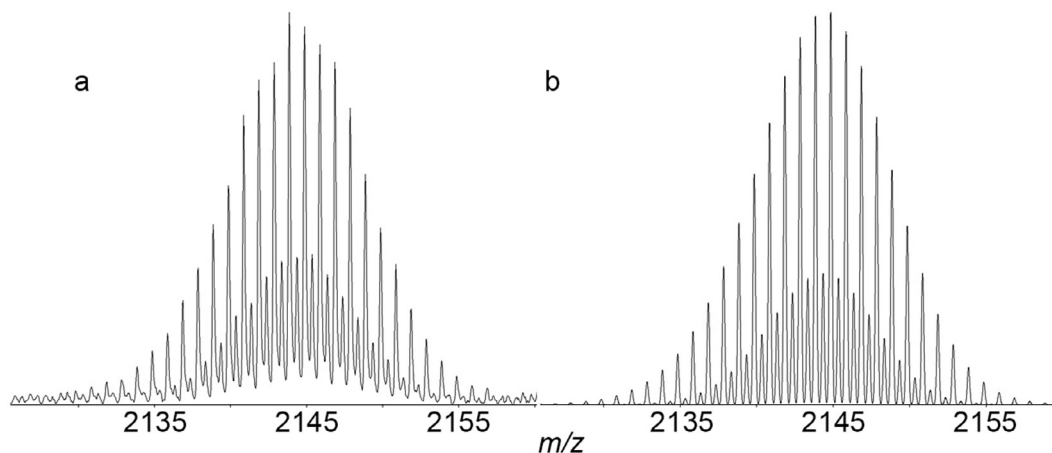
**Fig. 7.** (a) Experimentally-observed ion at $m/z$ 2144.80 and (b) calculated isotope pattern, modelled by combining isotope patterns of $[M]^+$ and $[2M]^{2+}$ in a ratio of 2:1 $[M]^+$: $[2M]^{2+}$ for $[M] = [\{Pt(PPh_3)\}_3(\mu_3\text{-Se})(\mu\text{-TePh})_3 + Se]$.

selected geometric parameters are collected in the figure caption. The structure comprises a cation and two independent anions, with each species having crystallographically imposed symmetry. The mono-cation is located on a crystallographic 3-fold axis in the trigonal space group $= R\bar{3}$, with the selenium atom lying on the axis. One $PF_6^-$ anion is also located on a 3-fold axis while the second is located on a site of symmetry, $\bar{3}$. Thus, the $3 \times 2/3^+$ charge of the cation is balanced by the $3 \times 1/3^-$ and $6 \times 1/6^-$ charges residing on the anions.

The selenium atom bridges three platinum(II) atoms located at the vertices of an equilateral triangle with Pt···Pt separations of 3.3565(5) Å. A $\mu_2$-bridging TePh ligand symmetrically spans each edge of the triangle with the resulting cyclic $[PtTe]_3$ arrangement having the form of a flattened chair. Each of the three platinum (II) atoms lies $-0.0694(2)$ Å above and each of the tellurium(II) atoms the same distance below the least-squares plane; the selenium(II) atom lies at the apex of a $SePt_3$ pyramid and 1.5988(9) Å above the aforementioned least-squares plane. The four-coordinate geometry for platinum(II) is completed by a $PPh_3$ ligand with the resulting $PSeTe_2$ donor set defining a distorted square planar geometry. This distortion is quantified by the respective deviations of the Te1, Te1$^i$, Se1 and P1 atoms of 0.1896(4), 0.1973(4), $-0.2068$(4), $-0.1800(4)$ Å from their least-squares-plane with the Pt atom lying 0.1975(5) Å out of the plane. Arguably, the most closely related structure in the literature is the all-sulfur analogue, where the selenium and tellurium atoms of **13b** are substituted by sulfur atoms, which was isolated as the chloride, acetone solvate [16]. The molecular structure of the cation resembles closely that in **13b** but, lacks the strict crystallographic symmetry of the latter. The Pt···Pt separations within the approximately equilateral triangle span a narrow range, i.e. 3.0440(6)–30609(9) Å, and are considerably shorter than in **13b** due, in part, to the formation of shorter Pt···$S_{apical}$ bond lengths, i.e. *ca.* 2.39 Å.

A view of the unit cell contents for **13b**·$PF_6$ is given in Fig. 8b. The ions comprising the structure are aligned in columns parallel to the unique axis, the c-axis, and are surrounded by the organic residues. Except for some weak phenyl-C—H···F interactions [38], the constituents are separated by van der Waals contacts.

## 2.5. Discussion and conclusion

The well-known affinity of platinum for chalcogen-containing ligands is exemplified by this study of the reactivity of the binuclear complexes $[Pt_2(\mu\text{-E})_2(PPh_3)_4]$ (E = S, Se) towards elemental chalcogens and diaryl dichalcogenides $R_2E_2$. This study has utilised the technique of ESI mass spectrometry for the convenient and data-rich exploration of the chemistry of the platinum sulfido and selenide complexes $[Pt_2(\mu\text{-E})_2(PPh_3)_4]$ towards a variety of chalcogen sources. ESI MS has been shown to be a powerful technique for exploring reaction chemistry, since it directly analyses the solution phase, miniscule amounts of sample are required, and there is generally a very good correlation between the ions observed in the MS analysis and the species present in solution [17]. In the chemistry of the $[Pt_2(\mu\text{-E})_2(PPh_3)_4]$ metalloligands, reaction products are often charged, and are thus ideally suited towards study by ESI MS. Using ESI MS we have been able to identify a wide range of interesting species in these reactions.

The facile reactions of **1** and **2** with diaryl dichalcogenides $Ph_2E_2$ result in the initial detection of an aryl-chalcogen adduct $[1 + EPh]^+$ or $[2 + EPh]^+$ (E = S, Se, Te). The reaction of diphenyl disulfide with $[Pt_2(\mu\text{-S})_2(PPh_3)_4]$ **1**, which ultimately resulted in the mono-derivatised phenylthiolato complex $[Pt_2(\mu\text{-S})(\mu\text{-SPh})(PPh_3)_4]^+$, identified the analogous intermediate $[Pt_2(\mu\text{-S})(\mu\text{-SSPh})(PPh_3)_4]^+$ [25]. Similarities with the reaction of $[Pt_2(\mu\text{-S})_2(PPh_3)_4]$ with $I_2$ were noticed, with $Ph_2S_2$ being compared to a mildly oxidising pseudohalogen [39].

After comparing reactions of diphenyl ditellurides with the parent sulfide and selenide complexes **1** and **2**, a proposed structure for a different trimetallic aggregate was elucidated in complexes **13a-d**. A complex of this type was also observed in the reaction of **1** with diphenyl diselenide. Initially unassigned, the ion observed at $m/z$ 1873 with an isotope pattern indicating a mono-cation and a composition of multiple polyisotopic elements, can be assigned as the trimetallic aggregate $[\{Pt(PPh_3)\}_3(\mu_3\text{-S})(\mu\text{-SePh})_3]^+$ (**10**, calculated $m/z$ 1873.01). Interestingly, no such trimetallic aggregate was observed in the reaction of **2** with diphenyl disulfide; instead trimetallic aggregates of the form $[Pt_3(\mu_3\text{-Se})_2(PPh_3)_5E_nPh]^+$ (E = S (n = 2); SeS (n = 1)) were observed.

The strength of the chalcogen-phenyl bond compared to the chalcogen-chalcogen bond in $Ph_2E_2$ has been reviewed in the literature [26,27] primarily for S and Se, with little data available for Te. Trends in bond dissociation energy (S—S > Se—Se > Te—Te; S—C > Se—C > Te—C) would suggest any Te—Te or Te—$C_{Ph}$ bonds to be much weaker than the corresponding bonds of the lighter chalcogens. This was specifically noticed with the assignment of the Ph-displaced species $[Pt_3(\mu_3\text{-S})_2(PPh_3)_5Ph]^+$, observed only in the reaction of **1** with diphenyl ditelluride.
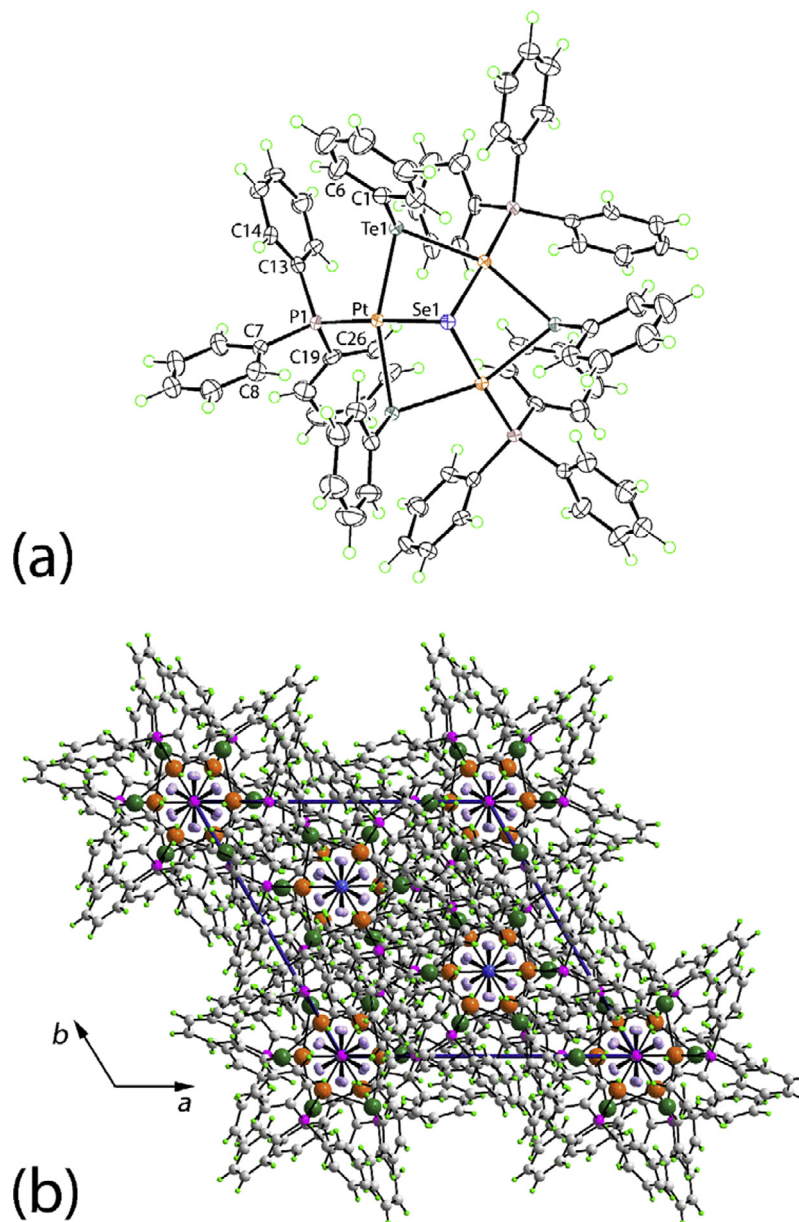
**Fig. 8.** (a) Molecular structure of the cation in **13b**·$PF_6$ showing atom labelling and 50 % probability displacement ellipsoids. The cation has crystallographic 3-fold axis and the unlabelled atoms are related by the symmetry operations (i) −x + y, −x, z or (ii) −y, −x − y, z. Selected geometric parameters: Pt–Te1 = 2.6128(4), Pt–Te1$^i$ = 2.6063(4), Pt–Se = 2.4687(6), Pt–P1 = 2.2501(13) Å; Te1–Pt–Te1$^i$ = 158.917(13), Te1–Pt–Se1 = 83.938(10), Te1–Pt–P1 = 98.58(4), Te1$^i$ –Pt–Se1 = 84.076(10), Te1$^i$ –Pt–P1 = 93.34(4), Se1–Pt–P1 = 177.41(3)°. (b) A view in projection down the c-axis of the molecular packing in **13b**·$PF_6$.

We are currently exploring the reactivity of $[Pt_2(\mu\text{-}E)_2(PPh_3)_4]$ towards a range of other Te sources, and results will be reported subsequently.

## 3. Experimental

### 3.1. Instrumentation

High-resolution ESI mass spectra were recorded using a Bruker MicrOTOF instrument. Calibration was periodically carried out using a methanolic solution of sodium formate. Spectra were recorded using either methanol or ethanol as the solvent; typically a drop of the reaction solution was diluted to *ca.* 1.5 mL with the solvent, and centrifuged to remove any insoluble matter prior to analysis. Typical parameters used a *Capillary Exit* voltage of 150 V and a *Skimmer 1* voltage of 50 V. Assignment of ions was assisted

by comparison of experimental and theoretical isotope patterns, the latter calculated using an internet-based program, or proprietary instrument-based software. Data were further analysed and prepared for presentation with the open-source mass spectrometry tool mMass [18].

### 3.2. Materials

The complexes $[Pt_2(\mu\text{-}S)_2(PPh_3)_4]$ **1** [40] and $[Pt_2(\mu\text{-}Se)_2(PPh_3)_4]$ **2** [6] were prepared by the literature procedures. The following compounds were used as supplied from commercial sources: diphenyl diselenide (Aldrich), diphenyl ditelluride (Aldrich), grey powdered selenium (BDH). ($p$-EtOC$_6$H$_4$)$_2$Te$_2$ was synthesised by the literature procedure [41]. Solvents used were of laboratory reagent grade.

Diphenyl disulfide was prepared by oxidation of thiophenol (BDH, 0.5 mL, 5 mmol) in MeOH (5 mL) with 27% $H_2O_2$ (1 mL, 10 mmol). After 1 h the white crystalline solid was filtered, washed with MeOH ($2 \times 10$ mL) and dried under vacuum (540 mg, 99%).

### 3.3. Attempted reaction of [Pt$_2$(μ-S)$_2$(PPh$_3$)$_4$] **1** with [Pt$_2$(μ-Se)$_2$(PPh$_3$)$_4$] **2** in methanol

[Pt$_2$(μ-S)$_2$(PPh$_3$)$_4$] (31 mg, 0.021 mmol) and [Pt$_2$(μ-Se)$_2$(PPh$_3$)$_4$] (29 mg, 0.018 mmol) were suspended in ethanol (20 mL), the mixture stirred at room temperature for 12 h, and analysed by positive-ion ESI MS.

### 3.4. Reaction of [Pt$_2$(μ-Se)$_2$(PPh$_3$)$_4$] **2** with S$_8$ in methanol

A mixture of [Pt$_2$(μ-Se)$_2$(PPh$_3$)$_4$] (30 mg, 0.019 mmol) and S$_8$ (5 mg, 0.020 mmol) in toluene (10 mL) and methanol (15 mL) was stirred at room temperature for 2 h resulting in a dark red-brown solution with a trace amount of insoluble matter. The solution was analysed by positive-ion ESI MS.

### 3.5. Reaction of [Pt$_2$(μ-S)$_2$(PPh$_3$)$_4$] **1** with elemental Se in ethanol

[Pt$_2$(μ-S)$_2$(PPh$_3$)$_4$] (40 mg, 0.027 mmol) and Se (100 mg, 1.27 mmol) were suspended in methanol (25 mL) and the mixture was stirred at room temperature for 48 h resulting in a black suspension. Centrifugation gave a light-yellow solution which was analysed by ESI MS.

### 3.6. Reaction of [Pt$_2$(μ-S)$_2$(PPh$_3$)$_4$] **1** with Ph$_2$Se$_2$

[Pt$_2$(μ-S)$_2$(PPh$_3$)$_4$] (25 mg, 0.017 mmol) and Ph$_2$Se$_2$ (15.5 mg, 0.05 mmol) were suspended in methanol (20 mL) and the resulting mixture stirred at room temperature for 24 h. The cloudy yellow mixture was filtered to remove any insoluble matter and the filtrate analysed by ESI MS. The reaction in ethanol was carried out in analogous fashion, using [Pt$_2$(μ-S)$_2$(PPh$_3$)$_4$] (30 mg, 0.020 mmol) and Ph$_2$Se$_2$ (19 mg, 0.061 mmol).

### 3.7. Reaction of [Pt$_2$Se$_2$(PPh$_3$)$_4$] **2** with Ph$_2$S$_2$ in methanol

[Pt$_2$(μ-Se)$_2$(PPh$_3$)$_4$] (25 mg, 0.016 mmol) and Ph$_2$S$_2$ (8.72 mg, 0.040 mmol) were suspended in methanol (20 mL) and the resulting mixture was stirred for 24 h. The cloudy dark-red mixture was filtered to remove any insoluble matter and the clear dark-red filtrate was examined by ESI MS. The reaction in ethanol was carried out in analogous fashion, using [Pt$_2$(μ-Se)$_2$(PPh$_3$)$_4$] (50 mg, 0.031 mmol) and Ph$_2$S$_2$ (13 mg, 0.060 mmol).

### 3.8. Reaction of [Pt$_2$(μ-Se)$_2$(PPh$_3$)$_4$] **2** with Ph$_2$Te$_2$ in ethanol

[Pt$_2$(μ-Se)$_2$(PPh$_3$)$_4$] (102 mg, 0.064 mmol) and Ph$_2$Te$_2$ (51.5 mg, 0.126 mmol) were suspended in ethanol (20 mL) and the mixture was stirred at room temperature for 48 h, giving a clear dark-red solution. The solution was analysed by positive-ion ESI MS.

### 3.9. Reaction of [Pt$_2$(μ-Se)$_2$(PPh$_3$)$_4$] **2** with (p-EtOC$_6$H$_4$)$_2$Te$_2$ in ethanol

[Pt$_2$(μ-Se)$_2$(PPh$_3$)$_4$] (98 mg, 0.061 mmol) and (p-EtOC$_6$H$_4$)$_2$Te$_2$ (62 mg, 0.125 mmol) were suspended in ethanol (20 mL) and the mixture was stirred at room temperature for 24 h, giving a clear dark-red solution. The solution was analysed by positive-ion ESI MS.

### 3.10. Reaction of [Pt$_2$(μ-S)$_2$(PPh$_3$)$_4$] **1** with diphenyl ditelluride in methanol

[Pt$_2$(μ-S)$_2$(PPh$_3$)$_4$] (51 mg, 0.034 mmol) and Ph$_2$Te$_2$ (27 mg, 0.066 mmol) were suspended in methanol (20 mL) and the mixture was stirred at room temperature for 48 h, giving a clear red-brown solution. The solution was analysed by positive-ion ESI MS.

### 3.11. Reaction of [Pt$_2$(μ-S)$_2$(PPh$_3$)$_4$] **1** with (p-EtOC$_6$H$_4$)$_2$Te$_2$ in methanol

[Pt$_2$(μ-S)$_2$(PPh$_3$)$_4$] (49 mg, 0.033 mmol) and (p-EtOC$_6$H$_4$)$_2$Te$_2$ (33 mg, 0.066 mmol) were suspended in methanol (20 mL) and the mixture was stirred at room temperature for 24 h, giving a clear dark-red solution. The solution was analysed by positive-ion ESI MS.

### 3.12. Synthesis of [{Pt(PPh$_3$)}$_3$(μ$_3$-Se)(μ-TePh)$_3$]PF$_6$ **13b**·PF$_6$

[Pt$_2$(μ-Se)$_2$(PPh$_3$)$_4$] **2** (102 mg, 0.064 mmol) and Ph$_2$Te$_2$ (51.5 mg, 0.126 mmol) were suspended in ethanol (20 mL) and the mixture was stirred at room temperature for 48 h, giving a clear dark-red solution. After filtration to remove trace amounts of insoluble matter, excess NH$_4$PF$_6$ (160 mg, 1 mmol) was added to the stirred filtrate producing a red-brown precipitate which was collected by vacuum filtration, washed successively with distilled water ($2 \times 10$ mL) and diethyl ether (5 mL), before drying under vacuum to give **13b**·PF$_6$ as a dark-brown solid (43.3 mg, 47%). ESI MS (positive-ion) $m/z$ 2065.98, 100%. Found: C 39.82, H 3.16. C$_{72}$H$_{60}$F$_6$P$_4$Pt$_3$SeTe$_3$ requires C 39.13, H 2.74%. Crystals suitable for an X-ray diffraction study were grown from an acetone/hexane solution.

### 3.13. X-ray crystallography

The diffraction data (19529 reflections; $\theta_{max}$ = 74.0°) for a diamond-like sample of [{Pt(PPh$_3$)}$_3$(μ$_3$-Se)(μ-TePh)$_3$]PF$_6$ **13b**·PF$_6$ (0.16 x 0.17 0.28 mm) were measured using a SuperNova CCD diffractometer with Cu-Kα radiation ($\lambda$ = 1.54184 Å) and ω scans. The intensity data were processed with the CrysAlis Pro software suite [42]; 4509 independent data ($R_{int}$ = 0.040) and 4072 with $I \geq 2\sigma(I)$. The structure was solved by direct methods [43] and full-matrix least-squares refinement on $F^2$ was performed using SHELXL-2014/7 [44] integrated in WinGX [45]. The C-bound H atoms were placed on stereochemical grounds and refined in the riding model approximation with $U_{iso} = 1.2U_{eq}$(carrier atom). A weighting scheme of the form $w = 1/[\sigma^2(F_o^2) + (0.0595P)^2 + 92.592P]$ where $P = (F_o^2 + 2F_c^2)/3$ was employed in the final cycles of refinement. Nine reflections were omitted from the final cycles of refinement as detailed in the CIF deposited with the CCDC (deposition number: 1520632). The maximum and minimum residual electron density peaks of 1.51 and 1.65 e Å$^{-3}$, respectively, were located 1.27 and 0.52 Å from the Te1 and P3 atoms, respectively. Crystallographic diagrams were drawn with ORTEP-3 for Windows [45] and DIAMOND [46]; PLATON [47] was also used in the study. Crystallographic data and refinement details for **13b**·PF$_6$: formula = C$_{144}$H$_{120}$F$_{18}$P$_9$Pt$_6$Se$_2$Te$_6$, formula weight = 2282.59, crystal system = trigonal, space group = $R\bar{3}$ (hexagonal setting), $a$ = 14.6495(4) Å, $c$ = 54.5424(17) Å, $V$ = 10137.0(6) Å$^3$, $Z$ = 3, $D_c$ = 2.243 g cm$^{-3}$, $\mu$ = 23.596 mm$^{-1}$, $R$ (obs. data) = 0.034, $R_w$ (all data) = 0.093.

## Acknowledgements

## Appendix A. Supplementary Material

CCDC 1520632 contains the supplementary crystallographic data for **13b**·PF6. These data can be obtained free of charge from The Cambridge Crystallographic Data Centre via www. ccdc.cam. ac.uk/data_request/cif.

## References

[1] R. Ugo, G. La Monica, S. Cenini, A. Segre, F. Conti, J. Chem. Soc. (1971) 522.
[2] C.E. Briant, C.J. Gardner, T.S.A. Hor, N.D. Howells, D.M.P. Mingos, J. Chem. Soc., Dalton Trans. (1984) 2645.
[3] M. Zhou, C.F. Lam, K.F. Mok, P.H. Leung, T.S.A. Hor, J. Organomet. Chem. 476 (1994) C32.
[4] For a review see, P. González-Duarte, A. Lledós, R. Mas-Ballesté, Eur. J. Inorg. Chem. (2004) 3585.
[5] S. Narayan, V.K. Jain, Transition Met. Chem. 25 (2000) 400.
[6] J.S.L. Yeo, J.J. Vittal, W. Henderson, T.S.A. Hor, J. Chem. Soc., Dalton Trans. (2001) 315.
[7] J.S.L. Yeo, J.J. Vittal, W. Henderson, T.S.A. Hor, Inorg. Chem. 41 (2002) 1194.
[8] J.S.L. Yeo, J.J. Vittal, W. Henderson, T.S.A. Hor, Organometallics 21 (2002) 2944.
[9] J.S.L. Yeo, J.J. Vittal, W. Henderson, T.S.A. Hor, J. Organomet. Chem. 659 (2002) 92.
[10] S.-W.A. Fong, T.S.A. Hor, J. Chem. Soc., Dalton Trans. (1999) 639.
[11] W. Henderson, T.S.A. Hor, Inorg. Chim. Acta 411 (2014) 199.
[12] V.K. Jain, L. Jain, Coord. Chem. Rev. 249 (2005) 3075.
[13] V.K. Jain, L. Jain, Coord. Chem. Rev. 254 (2010) 2848.
[14] W. Henderson, A.G. Oliver, Inorg. Chim. Acta 416 (2014) 49.
[15] S. Dey, V.K. Jain, B. Varghese, J. Organomet. Chem. 623 (2001) 48.
[16] C. Albrecht, S. Schwieger, C. Bruhn, C. Wagner, R. Kluge, H. Schmidt, D. Steinborn, J. Am. Chem. Soc. 129 (2007) 4551.
[17] W. Henderson, J.S. McIndoe, Mass Spectrometry of Inorganic, Coordination and Organometallic Compounds – Tools-Techniques-Tips, John Wiley & Sons, 2005.
[18] M. Strohalm, M. Hassman, B. Košata, M. Kodíček, Rapid Commun. Mass Spectrom. 22 (2008) 905.
[19] L.J. McCaffrey, W. Henderson, B.K. Nicholson, J.E. Mackay, M.B. Dinger, J. Chem. Soc., Dalton Trans. (1997) 2577.
[20] a) J.C. Bailar, H. Itatani, Inorg. Chem. 4 (1965) 1618;
b) A.R. Siedle, R.A. Newmark, P.A. Lyon, S.L. Hunt, V.W. Day, Inorg. Chim. Acta 259 (1997) 241;
c) M. Gomez, G. Muller, D. Sainz, J. Sales, X. Solans, Organometallics 10 (1991) 4036.
[21] B.C. White, D. Harrison, W. Henderson, B.K. Nicholson, T.S.A. Hor, Inorg. Chim. Acta 363 (2010) 2387.
[22] T.B. Nguyen, L. Ermolenko, W.A. Dean, A. Al-Mourabit, Org. Lett. 14 (2012) 5948.
[23] F. Lu, Inorg. Chem. Commun. 37 (2013) 148.
[24] J. Li, L.L. Koh, T.S.A. Hor, Chem. Commun. (2009) 3416.
[25] B.J. Deadman, W. Henderson, B.K. Nicholson, L.E. Petchell, S.L. Rose, T.S.A. Hor, Inorg. Chim. Acta 363 (2010) 637.
[26] Y. Guo, S.R. Alvarado, J.D. Barclay, J. Vela, ACS Nano 7 (2013) 3616.
[27] a) S. Antonello, R. Benassi, G. Gavioli, F. Taddei, F. Maran, J. Am. Chem. Soc. 124 (2002) 7529;
b) S. Płaza, R. Gruziński, Wear 194 (1996) 212.
[28] V.I. Tel'noy, M.S. Sheiman, Russ. Chem. Rev. 64 (4) (1995) 309.
[29] J.E. McDonough, J.J. Weir, M.J. Carlson, C.D. Hoff, O.P. Kryatova, E.V. Rybak-Akimova, C.R. Clough, C.C. Cummins, Inorg. Chem. 44 (9) (2005) 3127.
[30] R. Oilunkaniemi, R.S. Laitinen, M. Ahlgrén, J. Organomet. Chem. 623 (2001) 168.
[31] S.D. Apte, S.S. Zade, H.B. Singh, R.J. Butcher, Organometallics 22 (2003) 5473.
[32] J. Beckmann, S. Heitz, M. Hesse, Inorg. Chem. 46 (2007) 3275.
[33] P.C. Srivastava, S. Bajpai, R. Lath, R. Kumar, V. Singh, S. Dwivedi, R.J. Butcher, S. Hayashi, W. Nakanishi, Polyhedron 27 (2008) 835.
[34] A. Khanna, B.L. Khandelwal, A.K. Saxena, T.P. Singh, Polyhedron 14 (1995) 2705.
[35] R. Oilunkaniemi, R.S. Laitinen, M. Ahlgrén, J. Organomet. Chem. 595 (2000) 232.
[36] M.S. Hannu-Kuure, K. Palda'n, R. Oilunkaniemi, R.S. Laitinen, M. Ahlgrén, J. Organomet. Chem. 687 (2003) 538.
[37] J.G. Brennan, T. Siegrist, S.M. Stuczynski, M.L. Steigerwald, J. Am. Chem. Soc. 112 (1990) 9233.
[38] Short intermolecular C–H···F interactions in the molecular packing of **13b**·PF6: C15–H15···F3 = 2.54 Å, C15···F3 = 3.394(11) Å, angle at H15 = 150°; C21–H21···F1 = 2.33 Å, C21···F1 = 3.098(12) Å, angle at H21 = 133°; C21–H21···F1$^{iii}$ = 2.54 Å, C21···F1$^{iii}$ = 3.358(13) Å, angle at H21 = 145°. Symmetry operation (iii): ⅓+x−y, −⅔+x, ⅓−z.
[39] S.W.A. Fong, K. Evans, W. Henderson, B.K. Nicholson, T.S.A. Hor, Inorg. Chim. Acta 363 (2010) 301.
[40] W. Henderson, S. Thwaite, B.K. Nicholson, T.S.A. Hor, Eur. J. Inorg. Chem. (2008) 5119.
[41] a) R.L.O.R. Cunha, Á.T. Omori, P. Castelani, F.T. Toledo, J.V. Comasseto, J. Organomet. Chem. 689 (2004) 3631;
b) A. Chieffi, P.H. Menezes, J.V. Comasseto, Organometallics 16 (1997) 809.
[42] CrysAlis PRO, Rigaku Oxford Diffraction, Tokyo, Japan, 2015.
[43] G.M. Sheldrick, Acta Crystallogr., Sect. A 64 (2008) 112.
[44] G.M. Sheldrick, Acta Crystallogr., Sect. C 71 (2015) 3.
[45] L.J. Farrugia, J. Appl. Crystallogr. 45 (2012) 849.
[46] K. Brandenburg, DIAMOND, Crystal Impact GbR, Bonn, Germany, 2006.
[47] A.L. Spek, J. Appl. Crystallogr. 36 (2003) 7.